

Shear Thickening and Gel Elasticity in a Colloidal System with Attractive Interactions

Chinedum O. Osuji,* Chanjoong Kim, and David A. Weitz
School of Engineering and Applied Sciences, Harvard University Cambridge MA 02138
 (Dated: May 17, 2022)

Dilute oil dispersions of carbon black particles with attractive Van der Waals interactions display shear thickening in two distinct regimes. The first occurs at low shear rates, $\dot{\gamma}_{c1} \approx 10^0 \text{ s}^{-1}$ along with the formation of vorticity aligned shear-induced structures. The second high shear regime with $\dot{\gamma}_{c2} \approx 10^{2-3} \text{ s}^{-1}$ is driven by hydrodynamic breakup of clusters. Pre-shearing in the high rate shear thickening regime produces enhanced-modulus gels where $G' \sim \sigma_{pre-shear}^{1.5-2}$ and is directly proportional to the residual stress in the gel measured at a fixed sample age. The observed data can be accounted for using a simple scaling model for the breakup of fractal clusters under shear stress.

PACS numbers: 82.70.Dd, 83.80.Hj, 82.70.Gg

Colloidal particles interacting with attractive potentials in a fluid form gels above some critical volume fraction, $\phi > \phi_c$, where ϕ_c is a function of the interaction strength, U . The viscoelastic properties of such gels are determined by ϕ , U and the topology of the network of particle contacts, characterized by the fractal dimension of the network, d_f . Additionally, the properties are sensitive to the mechanical history of the system in question. To obtain reproducible results, rheological studies of colloidal gels typically employ a high rate pre-shear as a rejuvenation or initialization step in which the mechanical history of the gel is effectively erased. The non-Newtonian flow curves associated with attractive colloidal suspensions typically display monotonic shear thinning and as a result the modulus of the materials formed by gelation after pre-shear is not overly sensitive to the exact pre-shear flow condition. Shear thickening transitions are neither known nor predicted for these materials [1, 2]. Such transitions would be accompanied by drastic changes in the underlying fluid microstructure. As a result, the elasticity of gels would show a marked dependence on the nature of the pre-shear flow and its location on the flow curve relative to the shear thickening regime.

In this Letter we report on the observation of two regimes of shear thickening for attractive colloidal particles in a simple Newtonian fluid. We focus on the second, high shear rate region, and find that the elasticity of gels formed by pre-shearing in this regime scales as a power law with the pre-shear stress, and is directly proportional to the internal stress in the sample. We propose a scaling model which considers the dependence of the gel modulus on the cluster number density produced during the pre-shear flow. The model shows good agreement with the experimental data.

Measurements were performed at 25°C on dispersions of carbon black particles ranging from 2 to 8 wt.%. A non-polar, small-molecule fluid, tetradecane, was used as the suspending medium to avoid the complicating influences of electrostatics or adsorption of macromolecular

solvent species onto the colloidal surface. The carbon black (Cabot Vulcan XC72R) exists as $\approx 0.5 \mu\text{m}$ diameter fractal particles with fractal dimension $d_f^p = 2.2$ and $\rho_{carbon} = 1.8 \text{ g/cm}^3$. Tetradecane ($\rho_{solvent} = 0.762 \text{ g/cm}^3$, $\eta_{solvent} = 2.8 \text{ mPa}\cdot\text{s}$) was obtained from Aldrich Chemical Company. Samples were prepared by vigorous mixing of the two components using a vortexer. Optical studies were conducted using a Bohlin CS rheometer with a transparent base-plate through which microstructures were imaged using a CCD camera. Rheological measurements were carried out in strain-control mode using a TA Instruments AR-G2 rheometer with cone-plate and double-wall Couette geometries. The fast hardware-based feedback of the AR-G2 instrument, when run in strain-control, enabled measurements of the internal stress within samples by applying continuously computed torques to maintain constant tool position. Samples were pre-sheared before each measurement to remove the effect of shear history using an empirically determined shear rate which provided consistent results [3].

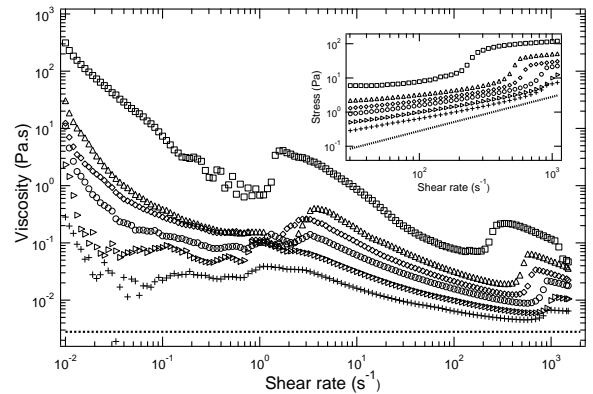


FIG. 1: Shear rate dependent viscosity for a series of weight fractions. + : 2%, > : 3%, o : 4%, < : 5%, Δ : 6%, □ : 8% The dotted-line is the background viscosity of the solvent. Inset: Rate dependent shear stress at the second shear thickening transition.

We measure the steady state viscosity as a function of shear rate using a cone-plate geometry. Initially, the gels exhibit shear thinning, but between $\approx 10^0$ and $10^1 s^{-1}$, there is a modest increase of viscosity, Figure 1. Optical studies using the plate-plate geometry show a build-up of structure in the sample via the formation of rolling, vorticity aligned cylindrical flocs in this regime. Such shear-induced structures have been observed in other viscoelastic systems under flow such as thixotropic clay gels [4], nanotube suspensions [5] and attractive emulsion droplets [6] but they have not previously been implicated in shear thickening [7]. Increasing shear rates result in additional shear thinning as the cylindrical flocs break down and form densified clusters, as in Figure 2a. This persists until $\approx 10^2 - 10^3 s^{-1}$ where there is a distinct transition to shear thickening flow. Shear thickening has in fact been reported [8], though not extensively considered, for a system consisting of carbon black particles in an adsorbing silicone oil. This was attributed to hydro-cluster formation due to the occurrence of stress overshooting at shear rates that produced shear thickening. In the present case, at high shear rates in the shear thickening regime, the system presents a finely dispersed microstructure in which the densified clusters produced at lower shear rates have been eroded. This results in a higher effective volume fraction of particles in the dispersion, and thus an enhanced viscosity, Figure 2b. In contrast to the hard sphere case, shear thickening results not from hydro-cluster formation, but from the breakup of locally dense clusters of the fractal colloidal particles into less dense structures which increase viscous dissipation in the system.

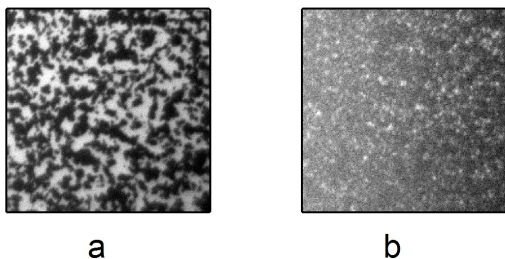


FIG. 2: Microstructure under shear in the parallel plate geometry. Gap size = $100\mu m$, $\phi = 3$ wt.% (a) 1.5×1.5 mm field of view, $\dot{\gamma} = 133 s^{-1}$ (b) 1.5×1.5 mm field of view, $\dot{\gamma} = 1330 s^{-1}$. To obtain sufficient light transmission through the optically dense sample in (b), the illumination was set several times higher than that used for (a). Binning of pixels on the CCD was used to decrease the required exposure time and so the resolution of image (b) is half that of (a).

Based on the dispersed particle size, we estimate the Péclet number, $Pe = \frac{\sigma a^3}{k_B T} \approx 10^2 - 10^3$, confirming that the high shear rate regime is dominated by hydrodynamic forces. Similarly, Reynold's number $Re = \frac{\rho \dot{\gamma} a^2}{\eta} \approx$

$10^{-4} - 10^{-5}$, indicating that viscous effects dominate and contributions from inertial forces should be minimal. Under similar conditions in Stokesian dynamics simulations of hard spheres [9, 10] a transition is observed from positive to negative normal forces on shear thickening due to hydrocluster formation at high Pe , with $|N_1| \sim \dot{\gamma}^1$ where N_1 is the normal stress. In the present system the normal stress transitioned sharply from small to large negative values at the onset of shear thickening, scaling as $|N_1| \sim \dot{\gamma}^2$ suggesting, along with the optical data, that hydrocluster formation is not in fact the mechanism in operation here. The critical shear rate at the onset of shear thickening, $\dot{\gamma}_c$, scales roughly as ϕ^β and the critical stress σ_c as ϕ^ν with β roughly between -1.5 and -2, and $\nu \approx 1$. From measurements performed using high viscosity basestock oil ($\eta \sim 33$ mPa.s), we observe that the critical shear rate is inversely proportional to the solvent viscosity, suggesting that shear thickening in this system is controlled by a critical stress, rather than by a critical rate.

We use dynamic measurements to study the dependence of the gel modulus on pre-shear flow and composition. Samples were sheared to remove the effects of flow history and then pre-sheared at the shear rate of interest for 20 minutes, more than sufficient to achieve a steady flow and constant viscosity. The system was then allowed to sit quiescently for 30 minutes. We measure the viscoelastic storage and loss moduli, G' and G'' , in the linear regime, $\gamma = 0.05\%$ at a fixed angular frequency $\omega = 1 rad/s$, where γ is the shear strain. The elastic or storage modulus of gels formed by pre-shearing at a fixed rate in the shear thickening regime follows a typical power law $G' \sim \phi^\alpha$, with exponent $\alpha = 3.5$, as might be expected for attractive systems [11]. In the shear-thinning regime, between the shear thickening transitions, the exponent is slightly higher, $\alpha = 4.2$. The elasticity of thickened gels is strongly enhanced, typically by over one order of magnitude, compared to gels produced in the non shear-thickening regime. The modulus follows the same qualitative dependence on shear rate as the viscosity, with a sudden upturn at the critical rate or critical shear stress. A double-wall Couette cell was used to mitigate the effects of sedimentation at low shear stresses where samples did not form robust thickened gels, or were too dilute to be gravitationally stable for study in the cone-plate geometry. Remarkably, as in Figure 3(inset), the dependence of the gel modulus on the pre-shear stress has a common form across different compositions, ϕ , such that the data can all be scaled onto a single curve using the critical stress, σ_c , and critical modulus, G'_c , as scaling parameters. Data located in the shear thickening regime show a striking dependence of the modulus on the pre-shear stress, $G' \sim \sigma^{1.5-2}$, as shown in Figure 3(main). These samples which were studied in the cone-plate geometry at large pre-shear stresses where the resulting high modulus gels were not sensitive to sedimen-

tation. There is a somewhat weaker volume fraction dependence such that in the shear thickening regime, overall, the modulus of the colloidal gel is largely determined by the pre-shear stress applied to the system prior to gelation.

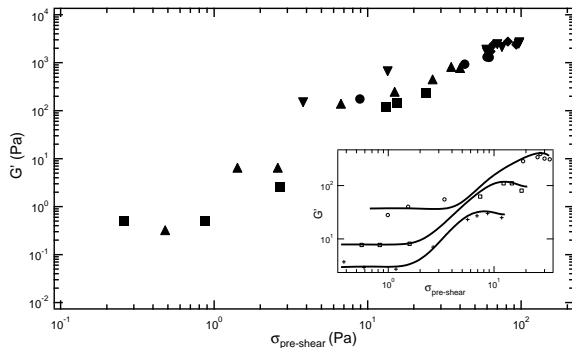


FIG. 3: Elasticity of shear thickened gels as a function of the pre-shear stress. \blacksquare : 3%, \blacktriangle : 4%, \bullet : 5%, \blacklozenge : 6%, \blacktriangledown : 8%. Inset: Data obtained at low stresses using a double-wall Couette cell. $+$: 2%, \square : 3%, \circ : 5%

We interpret these results in terms of the dependence of the cluster size on shear stress. As the stress increases, densified clusters break, and assume a size that is set by the balance between the shear stress and the cohesive energy density of the cluster.

The shear force on the cluster, $F_{shear} = 4\pi\sigma R_c^2$ where R_c is the radius of the fractal cluster. This force is spread across N_s particles in the plane of shear of the cluster where $N_s \sim R_c^{d_f-1}$ where d_f is the fractal dimension of the cluster. This force is balanced by the attractive interaction between particles, defined by the interaction strength $xk_B T$ and the relevant length scale, a , the particle diameter. Thus we have

$$R_c^{d_f-3} \sim \frac{4\pi\sigma a}{xk_B T} \quad (1)$$

which sets the dependence of the equilibrium cluster size on the shear stress. The elastic modulus scales directly with the number density of clusters. The number of clusters of radius R_c per unit volume scales as $\frac{\phi}{R_c^{d_f}}$ so that overall, we can expect the gel modulus to scale as

$$G' \sim \phi \sigma^{\frac{d_f}{3-d_f}} \quad (2)$$

For typical diffusion limited aggregation, $d_f \approx 1.8$ yielding $G' \sim \sigma^{3/2} \phi$. We plot this in Figure 4 and find good accord between our data and a slope of 1 as indicated, over several decades. Our scaling is in rough agreement with empirical data on flocculated systems which show that the number of particles in a floc or cluster, N_c scales roughly as $N_c \sim \sigma^{-1}$ [12].

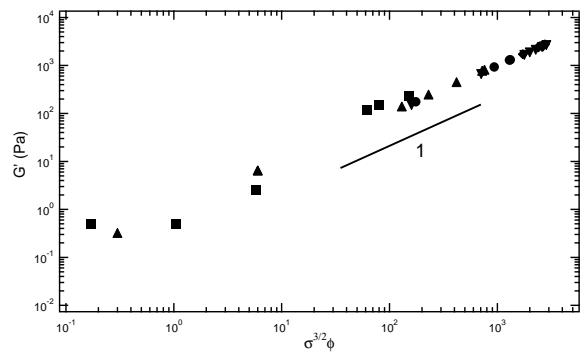


FIG. 4: Elasticity of shear thickened gels as a function of the pre-shear stress re-scaled according to equation (2) with $d_f = 1.8$. \blacksquare : 3%, \blacktriangle : 4%, \bullet : 5%, \blacklozenge : 6%, \blacktriangledown : 8%. The solid line is a visual guide with a slope of 1, showing good agreement of the model with the data.

The abrupt cessation of shear in a freely flowing colloidal system above the critical gelation composition ϕ_c results in a sudden entry into the gel state. The system loses mobility as particles experience sticky contacts with neighbors leading to the formation of structures that rapidly span space leading to an elastic medium. This rapid sol-gel transition should be characterized by the development of internal stresses coincident with the shear rate quench - the network structure, deformed with respect to an equilibrium relaxed configuration, would give rise to residual stresses which relax gradually over time. These internal stresses are believed to drive the slow dynamics observed in the aging of some glassy systems [13, 14]. Given that they result from a deformation of the structure, it is expected that such stresses should be proportional to the elastic modulus of the system [15], though no direct experimental evidence as yet confirms this. We measured the time dependent internal stresses in our samples from ~ 1 second after cessation of shear out to 30 minutes and find a weak power law decay of the stress with time over these periods. For shear thickened gels, the stress scales roughly as $\sigma_{internal} \sim t^{-0.2}$, inset Figure 5. The internal stress acts counter to the direction in which the sample was pre-sheared and is reversed on changing the pre-shear direction, indicating that the deformation of the clusters which gives rise to the internal stress occurs during shear and is locked in by the rate quench. Critically, we find that the internal stress at a fixed sample age, $t=30$ mins., is directly proportional to the modulus of the system measured immediately thereafter, over several orders of magnitude of internal stress, produced by different pre-shear flows, Figure 5. The prototypical picture of a slow diffusion limited gelation clearly does not apply despite the relatively low volume fractions under study here. Gelation is unusually rapid and the system displays a well developed elastic modulus at the shortest times studied, ≈ 1 second after cessation of shear.

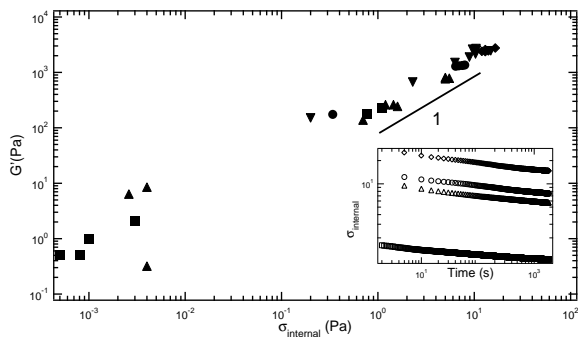


FIG. 5: Shear modulus scales linearly with residual stresses resulting from the quench into the gel state on cessation of flow. ■ : 3%, ▲ : 4%, ● : 5%, ◆ : 6%, ▼ : 8%. The solid line is a visual guide with a slope of 1. Inset: Time dependence of internal stress for 3, 4, 5 and 6 wt.%, plotted with open symbols for clarity.

Shear thickening in hard sphere and repulsive Brownian systems has been rationalized using a force balance model that compares the shear force pushing particles together to the diffusive flux that inhibits cluster formation [16].

$$\frac{3\pi\mu\dot{\gamma}_c a^3}{2h} = -k_B T \frac{\partial \ln g(r)}{\partial r} \quad (3)$$

where a is the particle radius, $h = r - 2a$ the distance between two particles, $g(r)$ the particle distribution function and μ the viscosity of the medium, replaceable by the suspension viscosity, η , as a way of accommodating many body effects. In the system under study here, at low shear stresses, large non-Brownian clusters resulting from breakage of the gel at low shear rates have no diffusive barrier towards further clustering. They densify as shear stresses force them into contact, reducing their effective volume fraction in the system. Above a critical stress however, the cohesive energy density of the clusters is overcome and they start to disintegrate with an attendant rise in viscosity.

The observation of shear thickening in this system of attractive particles was surprising. Indeed, previous careful examinations of flocculated systems have not resulted in observation of shear thickening [1, 2, 17]. A particularly systematic examination of the role of interaction strength using depletion forces [1] shows that shear thickening diminished and eventually disappeared on addition of substantial attractive interactions. Here, we observe shear thickening in 2 distinct regimes. It is clear that in this system the fractal nature of the particles, an irreversibly fused agglomerate of smaller particles produced by flame pyrolysis, plays a key role. Shear thickening is

a product of shear induced reduction of cluster size and increase of the effective volume fraction of the particles in the dispersion. Correspondingly, the modulus of shear thickened dispersions is enhanced due to the increase in cluster number density. The scaling of the elastic modulus with pre-shear stress is satisfactorily accounted for by consideration of the equilibrium cluster size as a function of this stress. The direct proportionality between the elastic modulus and the internal stress resulting from a system quench on cessation of shear has been confirmed by direct measurement. The dynamics of these internal stresses are a topic for continued studies.

The authors gratefully acknowledge L. Cipelletti, V. Trappe and H. Wyss for helpful discussions, and the Infineum Corporation for funding.

* chinedum.osuji@yale.edu; Present Address: Department of Chemical Engineering, Yale University, New Haven CT 06520

- [1] V. Gopalakrishnan and C. F. Zukoski, *Journal of Rheology* **48**, 1321 (2004).
- [2] S. R. Raghavan and S. A. Khan, *Journal of Colloid and Interface Science* **185**, 57 (1997).
- [3] V. Trappe and D. A. Weitz, *Physical Review Letters* **85**, 449 (2000).
- [4] F. Pignon, A. Magnin, and J. M. Piau, *Physical Review Letters* **79**, 4689 (1997).
- [5] S. Lin-Gibson, J. A. Pathak, E. A. Grulke, H. Wang, and E. Hobbie, *Physical Review Letters* **92**, 048302 (2004).
- [6] A. Montesi, A. A. Pena, and M. Pasquali, *Physical Review Letters* **92**, 058303 (2004).
- [7] C. O. Osuji and D. A. Weitz, to be published.
- [8] M. Kawaguchi, M. Okuno, and T. Kato, *Langmuir* **17**, 6041 (2001).
- [9] J. R. Melrose, J. H. vanVliet, and R. C. Ball, *Physical Review Letters* **77**, 4660 (1996).
- [10] A. Singh and P. R. Nott, *Journal of Fluid Mechanics* **412**, 279 (2000).
- [11] M. C. Grant and W. B. Russel, *Phys. Rev. E* **47**, 2606 (1993).
- [12] R. C. Sonntag and W. B. Russel, *Journal of Colloid and Interface Science* **113**, 399 (1987).
- [13] R. Bandyopadhyay, D. Liang, H. Yardimci, D. A. Sessoms, M. A. Borthwick, S. G. J. Mochrie, J. L. Harden, and R. L. Leheny, *Physical Review Letters* **93**, 228302 (2004).
- [14] M. Bellour, A. Knaebel, J. L. Harden, F. Lequeux, and J.-P. Munch, *Physical Review E* **67**, 031405 (2003).
- [15] L. Ramos and L. Cipelletti, *Physical Review Letters* **94**, 158301 (2005).
- [16] B. J. Maranzano and N. J. Wagner, *Journal of Rheology* **45**, 1205 (2001).
- [17] S. Raghavan, H. Walls, and S. Khan, *Langmuir* **16**, 7920 (2000).